

LAMOST Views δ Scuti Pulsating Stars

Qian S.-B.^{1,2,3,4}★ Li L.-J.^{1,2,3} He J.-J.^{1,2,3} Zhang J.^{1,2,3} Zhu L.-Y.^{1,2,3,4} and Han Z.-T.^{1,2,3}

¹Yunnan Observatories, Chinese Academy of Sciences (CAS), P. O. Box 110, 650216 Kunming, China

²Key Laboratory of the Structure and Evolution of Celestial Objects, Chinese Academy of Sciences, P. O. Box 110, 650216 Kunming, China

³Center for Astronomical Mega-Science, Chinese Academy of Sciences, 20A Datun Road, Chaoyang District, Beijing, 100012, P. R. China

⁴University of Chinese Academy of Sciences, Yuquan Road 19#, Sijingshang Block, 100049 Beijing, China.

Accepted XXX. Received YYY; in original form ZZZ

ABSTRACT

About 766 δ Scuti stars were observed by LAMOST by 2017 June 16. Stellar atmospheric parameters of 525 variables were determined, while spectral types were obtained for all samples. In the paper, those spectroscopic data are catalogued. We detect a group of 131 unusual and cool variable stars (UCVs) that are distinguished from the normal δ Scuti stars (NDSTs). On the H–R diagram and the $\log g - T$ diagram, the UCVs are far beyond the red edge of pulsational instability trip. Their effective temperatures are lower than 6700 K with periods in the range from 0.09 to 0.22 d. NDSTs have metallicity close to that of the Sun as expected, while UCVs are slightly metal poor than NDSTs. The two peaks on the distributions of the period and stellar atmospheric parameters are all caused by the existence of UCVs. When those UCVs are excluded, it is discovered that the effective temperature, the gravitational acceleration, and the metallicity all are correlated with the pulsating period for NDSTs and their physical properties and evolutionary states are discussed. Detection of those UCVs indicates that about 25% of the known δ Scuti stars may be misclassified. However, if some of them are confirmed to be pulsating stars, they will be a new-type pulsator and their investigations will shed light on theoretical instability domains and on the theories of interacting between the pulsation and the convection of solar-type stars. Meanwhile, 88 δ Scuti stars are detected to be the candidates of binary or multiple systems.

Key words: Stars: variables: Scuti – Stars: fundamental parameters – Stars: oscillations — Stars: binaries: general

1 INTRODUCTION

The δ Scuti-type pulsating stars lie inside the classical Cepheid instability strip with luminosity classes from III to V (e.g., Breger 1979, 2000; Lopez de Coca et al. 1990; Rodríguez et al. 2000). Their spectral types are in the range between A2 and F5 with masses from 3 to 1.4 M_{\odot} . The pulsating amplitudes are usually in the range of 0.003–0.9 mag in the V band, with periods usually between 0.02 and 0.3 d (e.g., Breger 1979; Chang et al. 2013). They exhibit both radial and non-radial pulsations with frequencies ranging between 3 and 80 d^{-1} and can oscillate in both p and g modes. These properties make them a good source for astroseismology investigations and thus study stellar interiors and stellar evolution. Their great number of radial and non-radial pulsation modes are mainly driven by the κ mechanism that is mostly working in the He II ionization zone (e.g., Gautschy & Saio 1995; Breger et al. 2005; Rodríguez & Breger 2001). The theoretical blue edge of δ Scuti instability trip was well determined (e.g., Pamyatnykh 2000),

while the red edge is rather complicated because of the coupling between convection and oscillation together with the turbulent viscosity (e.g., Xiong & Deng 2001). In the recent catalogue of δ Scuti pulsating stars, about 18 ones including VX Hya (F6) and DE Lac (F7) were reported to be beyond the red edge and thus have cool temperatures with the spectroscopic/photometric spectral types later than F5 (e.g., Chang et al. 2013).

A large number of δ Scuti stars were discovered by several photometric surveys in the world, e.g., All Sky Automated Survey (ASAS: Pojmanski 1997; Pojmanski et al. 2005), the asteroid survey LINEAR (Palaversa et al. 2013), and northern sky variability survey (NSVS: Woźniak et al. 2004). In particular, the Kepler (Borucki et al. 2010) space telescopes have produced high-quality data sets for thousands of stars and about 2000 δ Scuti stars were detected (e.g., Balona & Dziembowski 2011; Uytterhoeven et al. 2011). Since the data on variable stars including δ Scuti stars are constantly varying, the mission of VSX (the international variable star index) is bringing all of new information together in a single data repository (e.g., Watson et al. 2006). About 3689 δ Scuti variable stars have been detected and were listed in VSX by 2017 July

★ E-mail: qsb@ynao.ac.cn

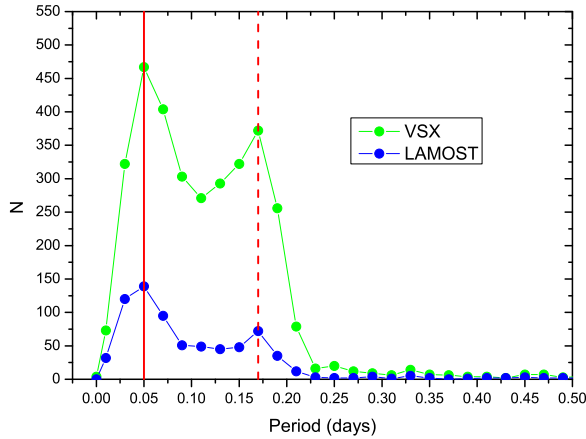


Figure 1. Period distributions of δ Scuti pulsating stars. Blue and Green dots represent δ Scuti variables observed by LAMOST and listed in VSX catalogue, respectively. Solid red line refers to the main peak near 0.05 d, while the dashed red line to the other small peak near 0.17 d.

16. Those photometric survey data are very useful to understand the photometric properties of δ Scuti variable stars. However, their spectroscopic information including spectral types and stellar atmospheric parameters extremely lacks. Among 1578 δ Scuti stars collected by Chang et al. (2013), only 15% of them have spectroscopic spectral types.

Large Sky Area Multiobject Fibre Spectroscopic Telescope (LAMOST, also called as Guo Shou Jing telescope) is a special telescope that has a field of view of 5 deg and could simultaneously obtain the spectra of about 4000 stars with low resolution of about 1800 in a one exposure (Wang et al. 1996; Cui et al. 2012). The wavelength range of LAMOST is from 3700 to 9000 Å and is divided in two arms, i.e., a blue arm (3700-5900 Å) and a red arm (5700-9000 Å). Huge amounts of spectroscopic data have been obtained for single stars and close binaries (e.g., Zhao et al. 2012, Luo et al. 2015; Qian et al. 2017a, b). In the time interval between 2011 October 24 and 2017 June 16, about 766 δ Scuti pulsating stars were observed by LAMOST. In the recent LAMOST data releases, stellar atmospheric parameters for 525 δ Scuti stars were determined when their spectra have higher signal to noise, while spectral types of all variables were obtained. Those spectroscopic data provide valuable information on their physical properties, evolutionary states, and binarities.

Among the 766 observed δ Scuti stars, the pulsating periods of 756 samples are given in VSX. The period distribution for those observed δ Scuti variables is shown in Fig. 1. Also displayed in the figure is the period distribution of δ Scuti variable stars listed in VSX where 339 δ Scuti stars without pulsating periods are not shown. The period distribution given by Rodriguez & Breger (2001) indicated that the majority of δ Scuti stars have short periods in the range from 0.05 to 0.1 d and the number is decreasing with increasing period. However, as shown in Fig. 1, there are two peaks in the period distributions. The main peak is near 0.05 d, while the other small peak is at 0.17 d. These properties are similar to those observed in RR Lyr-type pulsating stars (e.g., Szczygiel & Fabrycky 2007). The latter was caused by the known two types of RR Lyr-type pulsating stars, i.e., RRab and RRc. In the paper, we report

the detection of a group of unusual and cool variable stars (hereafter UCVs) that are distinguished from normal ones. Then, the physical properties of normal δ Scuti stars (hereafter NDSTs) are investigated after UCVs are excluded. Finally, based on the distributions of those atmospheric parameters and some statistical correlations, the physical properties, the binarities and the evolutionary states of δ Scuti stars are discussed.

2 CATALOGUES OF SPECTROSCOPIC OBSERVATIONS FOR UCVS AND NDSTs

In the latest LAMOST data releases, about 20.8% δ Scuti-type variables (766) listed in VSX were observed by LAMOST spectroscopic survey from 2011 October 24 to 2017 June 16. In the survey observations, every target was allocated to a fibre on the focal plane, and then be led into one of sixteen spectrographs equipped with thirty two $4K \times 4K$ CCDs [One spectrograph is equipped with two CCDs for recording blue (3700 A-5900 A) and red (5700 A-9000 A) wavelength regions, respectively]. Five flux standard stars were assigned to each spectrograph with highest priority for data reduction. The raw CCD data were reduced by the software called LAMOST 2D pipeline (Luo et al. 2015), which task includes dark and bias subtraction, flat-field correction, spectral extraction, sky subtraction, removing of telluric absorption, wavelength and relative flux calibration, and combination of red and blue wavelength regions. The extracted 1D spectra from 2D pipeline were then processed by the LAMOST 1D pipeline for their spectral classes (star, galaxy and QSO) as well as the spectral types and radial velocities of stars, or the redshifts of galaxies and QSOs. For the spectra of star from late A to FGK type, the LAMP (LAMOST Stellar Parameter Pipeline; Luo et al. 2015) is used to determine their atmospheric parameters (effective temperature T , surface gravity $\log g$, metallicity $[Fe/H]$, and radial velocity R_r). The two child components (CFI and ULYSS) in LAMP will be consecutively executed in an iterative way, and the final parameters are derived by ULYSS (Universite de Lyon Spectroscopic analysis Software; Koleva et al. 2009; Wu et al. 2011a) on the flux normalized spectra. The ULYSS determines the atmospheric parameters by minimizing the χ^2 between the observation and the model (Wu et al. 2011b). The model is cored by the TGM function which is an interpolator (Wu et al. 2011a) based on the empirical ELODIE stellar library (Prugniel & Soubiran 2001; Prugniel et al. 2007). Meanwhile, the model also employed a Gaussian broadening function characterized by the systemic velocity V_s , and the dispersion σ . This dispersion was contributed by both instrumental broadening and the projected rotational velocity of stars. The star rotation is taken into account coupled with the instrumental broadening, thus the rotational velocity itself cannot be derived as an output parameter.

Several independent works on comparing parameters between the earlier LAMOST data release and other reliable spectral data bases, such as high resolution spectral results, SDSS, APOGEE, and PASTEL, were carried out and described by Luo et al (2015). The typical standard deviations from these comparisons are 95 K for T , 0.25 dex for $\log g$, 0.1 dex for $[Fe/H]$, and 7 km/s for R_r . For the latest LAMOST data (DR4 and the first three quarters of DR5) used in this work, the same comparisons are required. To this aim we compared the LAMP data with those mainly derived from high-resolution optical spectra from the literature by Frasca et al. (2016). The comparisons are plotted in the four panels of Fig. 2 where the stellar atmospheric parameters of 352 stars are shown. We note that there are very good agreements for those four param-

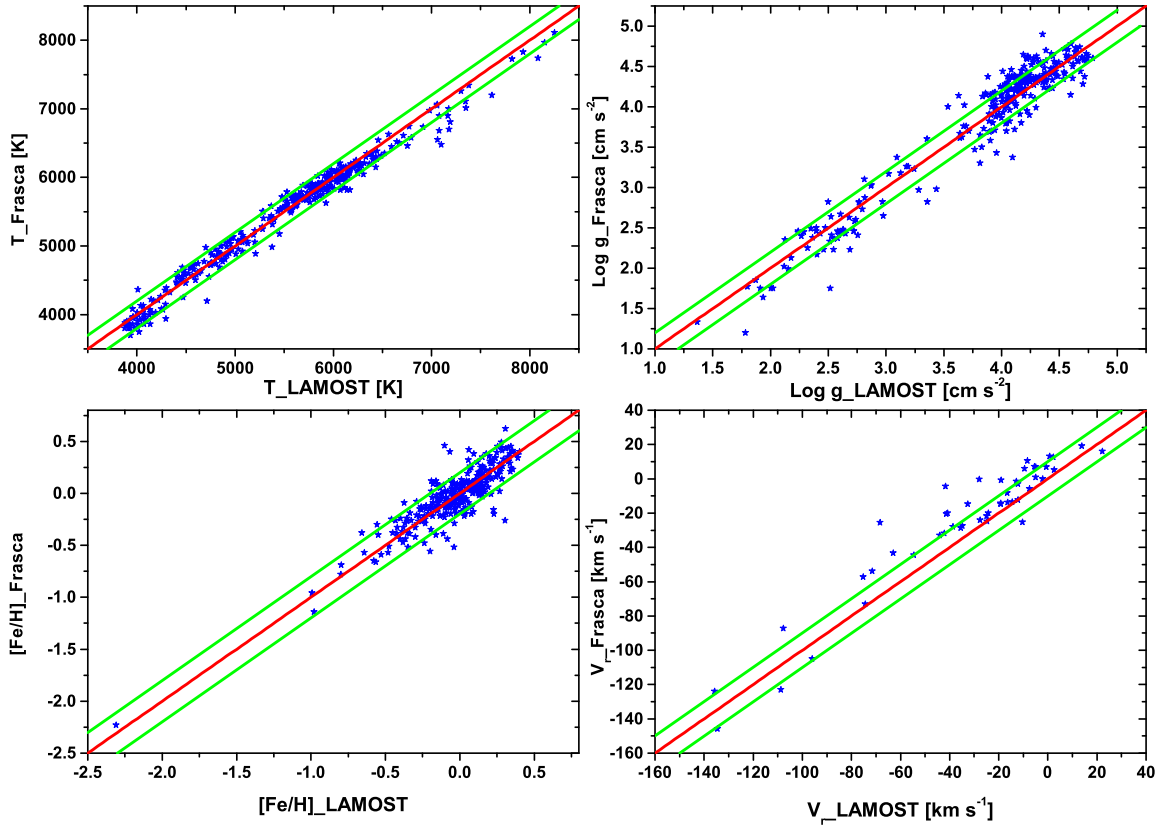


Figure 2. Comparison between LAMP data with literature values based mainly on high resolution spectra. The red solid lines are the one-to-one relationships. The green lines in the four panel refer to a difference of 200 K for T , 0.2 for $\log g$ and $[\text{Fe}/\text{H}]$, and 10 km s^{-1} for V_r , respectively.

eters. The dashed blue lines in those panels refer to a difference of 200 K for T , 0.2 for $\log g$ and $[\text{Fe}/\text{H}]$, and 15 km/s for V_r , respectively. Most of the targets are within the differences. The standard deviations are derived as 135 K for T , 0.21 dex for $\log g$, 0.14 dex for $[\text{Fe}/\text{H}]$, and 11 km/s for V_r .

About 2000 δ Scuti variables were found by the Kepler space telescope (e.g., Balona & Dziembowski 2011; Uytterhoeven et al. 2011). Some of them were also observed by LAMOST from 2011 October 24 to 2017 June 16. They were included in the LAMOST-Kepler project (e.g., Frasca et al. 2016; Gray et al. 2016; Ren et al. 2016). Based on the LAMOST spectra, the atmospheric parameters for tens of thousands of stars in the Kepler field were determined by Frasca et al. (2016) with the code ROTFIT that was developed by Frasca et al. (2003, 2006). Stellar atmospheric parameters of 188 δ Scuti stars were obtained. The comparisons between the present atmospheric parameters of the 188 LAMOST-Kepler δ Scuti stars with those derived with ROTFIT are shown in Fig. 3 where the red solid lines in the four panel represent the one-to-one relationships. The dashed blue lines refer to a difference of 200 K for T , 0.2 for $\log g$ and $[\text{Fe}/\text{H}]$, and 15 km/s for V_r , respectively. It is shown that there is a good agreement for the effective temperature. As for $\log g$, apart from a few targets, most δ Scuti stars are within the difference. The $[\text{Fe}/\text{H}]$ values are only in good agreement with the ROTFIT

data when $[\text{Fe}/\text{H}] < 0.3$. As for the radial velocity, most δ Scuti stars are also within the difference of 15 km/s although the ROTFIT data tend to have lower values for some targets.

The temperatures of all targets are below 8500 K, their atmospheric parameters could be determined well. Among the 766 δ Scuti stars, stellar atmospheric parameters of 525 δ Scuti stars were determined by using good and reliable spectra. Their atmospheric parameters were automatically determined by ULYSS (e.g., Koleva et al. 2009; Wu et al. 2011a, b, 2014; Luo et al. 2015). There are 32 δ Scuti variable stars observed four times or more on different dates. To check the reliability of stellar atmospheric parameters, we determined the mean values of their atmospheric parameters and derived the corresponding standard errors. The results are shown in Table 1, where their names and pulsating periods are listed in the first and the second columns. The observational times are shown in third column, while the average atmospheric parameters and their standard errors are displayed in the rest columns. As shown in Table 1, apart from two targets, the standard errors of the effective temperature for the rest targets are lower than 100 K. As for the gravitational acceleration $\log g$, apart from one target, the standard errors of the others are lower than 0.1 dex, while the standard errors of the metallicity for most δ Scuti variable star targets are lower than 0.08 dex. These results are consistent with the standard deviations determined by

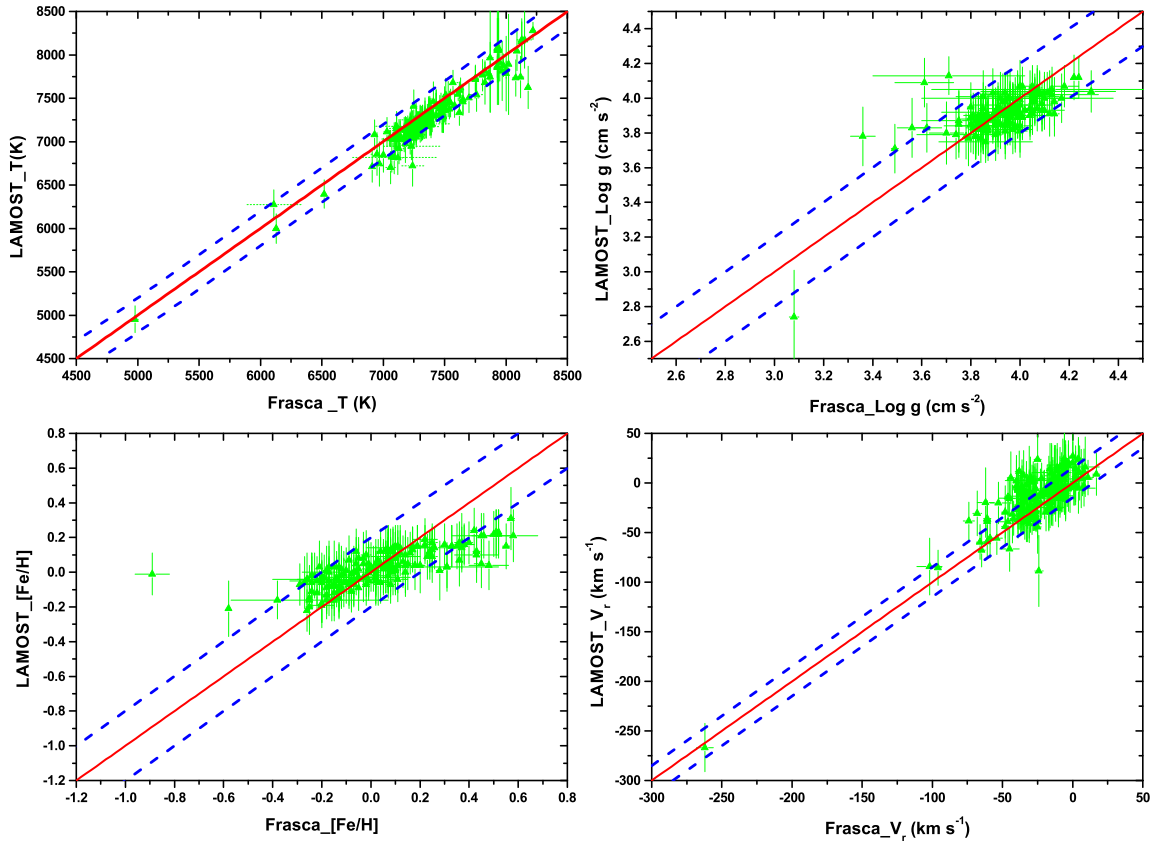


Figure 3. Comparison between LAMOST atmospheric parameters of LAMOST-Kepler δ Scuti stars with those derived with ROTFIT from the LAMOST spectra by Frasca et al. (2016). As those in Fig. 2, the red solid lines in the four panel are the one-to-one relationships. The dashed blue lines refer to a difference of 200 K for T , 0.2 for $\log g$ and $[\text{Fe}/\text{H}]$, and 15 km s^{-1} for V_r , respectively.

comparing LAMOST data with those derived from high-resolution spectra. This indicates that the present data for those δ Scuti stars are reliable.

The correlation between the pulsating period P and the effective temperature T for those observed δ Scuti stars is displayed in Fig. 4. The pulsating periods in the figure are from VSX¹ (e.g., Watson, 2006). As shown in Fig. 4, there is a group of 131 UCVs (green dots) that are clearly separated from the other 394 variable stars (blue dots) indicating that they are a new group of unusual variable stars. The dashed red lines in the figure represent the borders of UCVs. Their temperatures are lower than 6700 K and the periods are in the range from 0.09 to 0.22 d. Four targets, KIC 9700679 ($P=3.81679$ d), KIC 5446068 ($P=3.48432$ d), BOKS-24178 ($P=0.7$ d), and $BD + 19^{\circ}572$ (without period), with temperatures below 6700 K are not shown in the figure because their periods are not in the range. The atmospheric parameters of the 131 UCVs including the effective temperature T , the surface gravity $\log g$, and the metallicity $[\text{Fe}/\text{H}]$ are listed in Table 2 in the order of increasing VSX number. When some of them were observed twice

or more times on different dates, the atmospheric parameters are averaged and the corresponding standard errors are given. Those listed in Table 2 are the first 20 sets of observations. The whole table is available in the internet electronic version² and it will be improved by adding new data obtained by LAMOST in the future. Table 2 includes star names, their right ascensions (RA) and declinations (DEC), and pulsating periods. These parameters are from VSX catalogue. When the targets are observed two times or more, the effective temperature T , the gravitational acceleration $\log g$ and the metallicity $[\text{Fe}/\text{H}]$ are averaged and the weight of each value is the inverse square of the original error. The mean spectral types are listed in columns 5 and those shown in columns 6 and 7 are observational dates and times (N). Only the first date and the last date are given in the table as the targets were observed more than two times. The stellar atmospheric parameters including T , $\log g$, and $[\text{Fe}/\text{H}]$, are listed in columns 8, 10, and 12, while their corresponding errors are displayed in columns 9, 11, and 13, respectively. The stellar atmospheric parameters of the other 394 NDSTs are shown in Table 3 in the order of increasing VSX number. The arrangement

¹ <http://www.aavso.org/vsx/>

² <http://search.vbscn.com/DSCT.Table2.txt>

Table 1. Mean stellar atmospheric parameters for 32 δ Scuti stars observed 4 times or more and their standard errors.

Star name	Period (d)	N	\bar{T} (K)	Errors	log g	Errors	[Fe/H]	Errors
KIC 10014548	0.65445	11	7210	18	3.82	0.03	0.56	0.02
KIC 7697795	0.057185	10	7498	11	3.86	0.01	0.08	0.01
KIC 7106205	0.074655	10	7167	15	3.85	0.02	0.12	0.01
KIC 11395392	0.039701	7	7261	45	4.13	0.02	-0.25	0.02
KIC 9391395	0.51308	7	7243	11	4.05	0.01	-0.20	0.01
KIC 8149341	0.037015	7	7505	32	3.84	0.04	0.16	0.02
KIC 3942911	0.03391	6	7438	21	3.96	0.02	0.05	0.02
KIC 8747415	0.090662	6	4989	30	3.10	0.04	-0.18	0.03
ASAS J075941-0353.1	0.180982	6	7073	32	3.75	0.03	0.18	0.02
KID 07900367	0.075489	5	7198	16	3.80	0.02	0.51	0.00
KIC 9324334	0.097352	5	7238	27	3.96	0.03	0.13	0.02
KIC 10615125	0.10351	5	7202	13	3.83	0.01	0.35	0.01
KIC 11127190	0.053387	5	7448	16	3.92	0.01	0.26	0.01
KIC 9700679	3.81679	5	5451	82	3.09	0.10	0.06	0.08
BW Cnc	0.072	5	7421	40	3.90	0.02	0.13	0.01
KIC 8869892	0.12989	4	7068	22	3.89	0.09	-0.10	0.13
BD+24 95	0.11992	4	7090	22	3.75	0.01	0.49	0.02
KIC 10002897	0.064965	4	7305	17	4.06	0.01	-0.10	0.05
GSC 01946-00035	0.067081	4	7265	40	4.00	0.01	-0.03	0.03
ASAS J190751+4629.2	0.079561	4	7180	8	3.92	0.03	0.19	0.01
V0367 Cam	0.121596	4	7308	126	3.86	0.02	0.19	0.05
ASAS J064626+2629.8	0.205972	4	6613	10	4.16	0.03	-0.25	0.01
ASAS J071540+2022.2	0.200724	4	6308	5	4.17	0.01	-0.08	0.02
KIC 10208345	0.28969	4	7146	24	4.00	0.04	-0.08	0.03
KIC 10065244	0.083822	4	7114	23	3.97	0.02	-0.03	0.02
KIC 9775385	0.55928	4	7360	8	3.98	0.01	0.07	0.01
KIC 7668791	0.048443	4	8197	12	3.83	0.01	-0.08	0.01
KIC 7350486	0.75188	4	7132	11	3.89	0.02	0.10	0.01
KIC 7109598	0.053772	4	7275	45	3.87	0.04	0.36	0.03
KIC 5446068	3.48432	4	6200	311	3.99	0.27	0.29	0.02
KIC 4488840	0.063279	4	7275	26	3.93	0.01	0.06	0.02
BS Cnc	0.051	4	7480	18	3.91	0.02	0.06	0.01

Table 2. Stellar atmospheric parameters for the 131 UCVs detected by LAMOST (the first 20 lines of the whole table).

Name	R.A. (deg)	Dec. (deg)	Period (d)	Sp.	Dates	N	T (K)	E_1	log g	E_2	[Fe/H]	E_3
GM Com	183.1038	27.38008	0.208	F3	2011-12-21–2011-12-21	1	6680	20	4.15	0.02	-0.10	0.02
ASAS J001921+0127.1	4.83683	1.45297	0.156951	G7	2012-10-29–2012-10-29	1	5260	30	3.74	0.03	0.05	0.02
ASAS J010045+2648.4	15.18808	26.80683	0.190532	F2	2015-10-31–2015-10-31	1	5980	10	4.32	-	-0.59	-
ASAS J011159+2548.8	17.99496	25.81331	0.157222	F6	2014-10-25–2014-10-25	1	5980	290	3.88	0.41	-0.51	0.27
ASAS J011208+0217.2	18.03254	2.28617	0.176614	G5	2012-10-31–2016-12-30	2	5761	5	4.31	0.01	0.10	0.01
ASAS J011959+1500.4	19.99579	15.00731	0.199153	F9	2016-01-19–2016-01-19	1	6000	20	4.12	0.02	0.11	0.01
ASAS J012334+2108.6	20.89288	21.14336	0.185343	F4	2012-12-03–2014-11-19	2	6020	55	4.03	0.07	-0.24	0.05
ASAS J013458+0553.2	23.74217	5.88589	0.164786	F9	2015-12-11–2015-12-11	1	5960	320	4.44	0.45	-0.43	0.29
ASAS J020653+0815.6	31.71892	8.26008	0.177637	G3	2012-09-29–2012-09-29	1	5550	100	3.82	0.14	-0.34	0.09
ASAS J022414+2741.6	36.05646	27.69336	0.155998	G3	2013-10-06–2017-01-28	2	5713	5	4.26	0.01	-0.05	0.00
ASAS J030054+2301.7	45.22333	23.02756	0.181652	G2	2015-10-30–2015-10-30	1	5850	90	4.31	0.12	-0.04	0.08
ASAS J030701+1534.2	46.75504	15.56981	0.171276	F2	2012-09-30–2012-09-30	1	6060	20	4.15	0.02	-0.15	0.01
ASAS J030858-0251.8	47.23971	-2.86344	0.135452	K3	2017-02-06–2017-02-06	1	5106	42	4.43	0.06	-0.29	0.04
ASAS J032314+0406.0	50.80875	4.10236	0.157606	F2	2014-12-02–2014-12-02	1	6049	100	4.11	0.14	-0.20	0.09
ASAS J034144+1638.1	55.43454	16.63453	0.163976	F6	2016-12-19–2016-12-19	1	6027	7	4.26	0.01	-0.42	0.01
ASAS J035613+2600.1	59.05558	26.00178	0.195533	F5	2016-11-10–2016-11-10	1	6345	2	4.14	0.00	-0.05	0.00
ASAS J040216-0321.7	60.56533	-3.36314	0.155724	K3	2012-11-01–2012-11-01	1	4960	60	4.27	0.08	0.31	0.05
ASAS J041458+0501.2	63.7415	5.01972	0.170028	F0	2015-11-29–2015-11-29	1	6320	10	4.19	-	-0.55	-
ASAS J052412+0020.2	81.05208	0.33606	0.196369	F5	2014-11-18–2014-11-18	1	6360	20	4.11	0.02	-0.21	0.01
ASAS J053125+1103.8	82.85413	11.06303	0.144799	F5	2013-10-02–2014-12-10	2	5948	8	4.08	0.02	-0.43	0.01

of the table is the same as those in Table 2 where only the first 20 observations are shown in Table 3 (the whole table is available via the internet electronic version³).

For some δ Scuti stars, their spectra signals to noise are not high enough to determine the stellar atmospheric parameters and thus only spectral types were given. The spectral types of those δ Scuti variable stars are catalogued in an electronic table where 588

³ <http://search.vbscn.com/DSCT.Table3.txt>

Table 3. Catalogue of NDSTs observed by LAMOST (the first 20 observations).

Name	R.A. (deg)	Dec. (deg)	Period (days)	Sp.	Dates	N	T (K)	E_1	$\log g$	E_2	[Fe/H]	E_3
GP And	13.82563	23.16372	0.078683	F0	2013-10-15–2013-10-15	1	7200	40	4.11	0.06	-0.41	0.04
YZ Boo	231.0292	36.86683	0.104092	A7	2015-02-18–2015-03-09	2	7306	8	4.05	0.01	-0.29	0.01
BS Cnc	129.7879	19.59239	0.051	A7	2015-03-08–2016-02-24	4	7471	6	3.89	0.01	0.07	0.01
BV Cnc	130.1373	19.19433	0.21	A9	2015-10-30–2016-02-24	2	7325	7	3.95	0.02	0.23	0.01
BW Cnc	130.2187	20.26653	0.072	A8	2015-03-08–2017-02-13	5	7421	4	3.90	0.00	0.13	0.00
GP Cnc	129.5405	7.22583		F0	2015-02-06–2015-02-06	1	7320	10	4.12	0.01	-0.39	0.01
V0927 Her	254.075	50.12664	0.130528	F0	2017-05-16–2017-05-16	1	7169	7	3.83	0.01	0.19	0.01
UX LMi	161.4258	27.96506	0.15064	F0	2011-12-15–2011-12-26	2	7049	9	3.67	0.01	0.44	0.01
WW LMi	163.6757	25.49072	0.12691	F0	2012-01-04–2012-03-11	2	7220	14	3.77	0.02	0.30	0.01
V0501 Per	63.96912	51.21828		F0	2012-02-08–2012-02-08	1	7140	140	4.26	0.19	-0.14	0.12
UV Tri	23.00046	30.36569		F0	2013-10-04–2013-10-04	1	7250	20	3.89	0.02	0.14	0.01
V0460 And	38.55942	42.241	0.074981	A6	2014-11-04–2014-11-04	1	8120	40	4.16	0.05	-0.25	0.03
NSV 1273	56.39346	24.46328		A6	2016-09-30–2016-11-10	2	7297	2	4.08	0.00	-0.10	0.00
V1116 Her	247.5683	16.91833	0.094683	A7	2013-04-20–2013-04-20	1	7750	10	4.12	-	-0.41	-
NSV 12196	293.8245	46.419	0.052768	A7	2012-06-04–2012-06-04	1	7430	10	3.91	-	0.09	-
NSV 19942	205.9122	21.0957	0.16352	F0	2015-01-23–2017-06-07	3	7099	22	3.72	0.03	0.45	0.02
V0478 And	4.73279	22.66117	0.096	F0	2016-12-04–2016-12-04	1	7398	3	3.96	0.00	-0.09	0.00
ASAS J012242+0854.1	20.67687	8.90192	0.067416	A7	2015-12-11–2015-12-11	1	7379	30	4.18	0.03	-0.45	0.02
ASAS J024816+2213.4	42.06658	22.22214	0.080315	F0	2015-01-18–2015-01-18	1	7290	10	3.89	-	0.01	-
ASAS J030012+0731.1	45.05079	7.51789	0.067219	A5	2012-11-01–2012-11-01	1	7440	10	4.14	0.01	-0.44	0.01

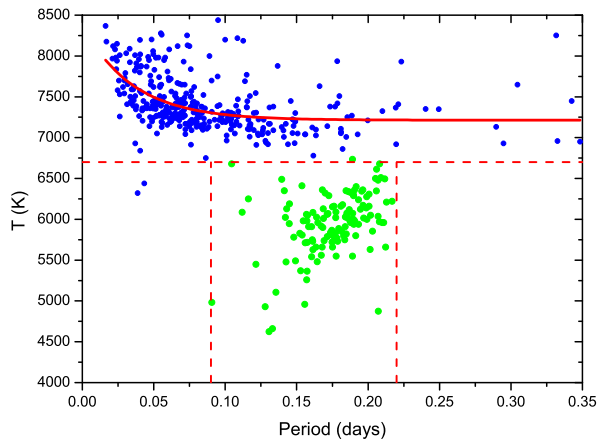


Figure 4. Correlation between the pulsating period and the effective temperature for δ Scuti variable stars with periods shorter than 0.35 d. A group of 131 UCVs (green dots) is shown to be distinguished from the normal ones (blue dots). The dashed red lines represent their borders. The UCVs have temperatures lower than 6700 K with pulsating periods in the range from 0.09 to 0.22 d. The solid red line indicates that there is a good relation between the period and the effective temperature for normal δ Scuti stars with period shorter than 0.35 d.

spectral types are listed. This table is available at the website⁴ via the internet. For about 241 δ Scuti stars, only spectral type was obtained by LAMOST. Both spectral types and stellar atmospheric parameters were determined for 525 δ Scuti stars. In order to provide more information to the readers, the original LAMOST stellar parameter for UCVs and NDSTs are also included in the table. In total, 182 sets of spectroscopic observations for 131 UCVs and 661 sets of data for 394 NDSTs are also catalogued in this table

⁴ <http://search.vbscn.com/DSCT.LAMOSTdata.txt>

that contains 16 columns. As those shown in Tables 2 and 3, the first three columns include the star names, their right ascensions RA and declinations DEC. The types of light variation and pulsating periods are listed in columns 4 and 5. These parameters are from VSX catalogue. The types of light variation are defined in the GCVS variability classification scheme⁵ (e.g., Samus et al. 2017). Column 6 lists the distances (in arcsec) between the two positions determined by the coordinates given in VSX and by LAMOST. As pointed by Qian et al. (2017a), the distances were used to identify those δ Scuti variable stars from the LAMOST samples based on the criterion $\text{Dist} < 2$ arcsec. For most of the targets, the values of Dist are smaller than 0.1 arcsecs. However, the Dist values of several δ Scuti are larger than 1 arcsec. We have checked their stellar charts by using the coordinates given in VSX and by LAMOST. It is shown that they are the same stars and their results are not for different objects. The differences may be caused by the fact that the coordinates for a few targets are not given in high precision. The observing dates are shown in column 7, while the determined spectral types are listed in column 8. The stellar atmospheric parameters including T , $\log g$, [Fe/H], and V_r , are listed in columns 9, 11, 13, and 15. Their corresponding errors E_1 , E_2 , E_3 , and E_4 are also displayed in the table, respectively.

3 DISTRIBUTIONS OF STELLAR ATMOSPHERIC PARAMETERS AND BINARITIES FOR δ SCUTI VARIABLES

As aforementioned, the stellar atmospheric parameters of 525 δ Scuti pulsating stars were determined. In this section, we investigate the properties of the δ Scuti stars by using those spectroscopic data listed in Tables 2 and 3. During the analyses, when the δ Scuti variables were observed two times or more by LAMOST, the weighted mean values of all individuals are used and the weight is the inverse square of the original error from each observation. As for the radial velocity V_r , we do not average them and use the individual values. The distribution of the effective temperature for

⁵ <http://www.sai.msu.su/gcvs/gcvs/iii/vartype.txt>

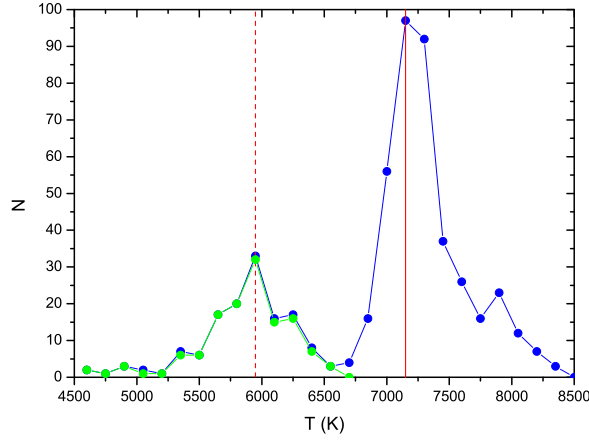


Figure 5. Distribution of the effective temperature for whole δ Scuti variable stars whose stellar atmospheric parameters were determined by LAMOST (blue dots). The solid red line refers to the main peak near 7150 K, while the dashed red line to the small peak near 5950 K. The temperature distribution for the 131 UCVs (green dots) is also plotted. It is shown that the small peak is constructed by the existence of the group of cool variable stars.

Table 4. 10 δ Scuti variable stars with the highest metallicities.

Name	$\alpha(2000)$	$\delta(2000)$	Period (d)	Sp.	T (K)	$\log g$	[Fe/H]	V_r (km s $^{-1}$)
V2703 Cyg	302.0067	30.87896	0.1166	F0	7100	3.74	0.60	-3
KIC 10014548	293.0593	46.90581	0.65445	F0	7206	3.83	0.56	-64
KID 07900367	294.9373	43.69592	0.075489	F0	7198	3.8	0.51	-24
KIC 8103917	294.0302	43.91889	0.056348	F0	7310	3.82	0.49	-27
KIC 9874181	282.8607	46.78	0.049222	F0	7440	3.81	0.49	-29
BD+24 95	10.26	25.26081	0.11992	F0	7092	3.75	0.49	-20
KIC 4936524	295.2013	40.04136	0.035665	F0	7391	3.83	0.46	-7
NSV 19942	205.9122	21.0957	0.16352	F0	7099	3.72	0.45	6
KIC 5722346	296.3865	40.94497	0.0883	F0	7130	3.90	0.45	-15
UX LMi	161.4258	27.96506	0.15064	F0	7050	3.67	0.44	-8

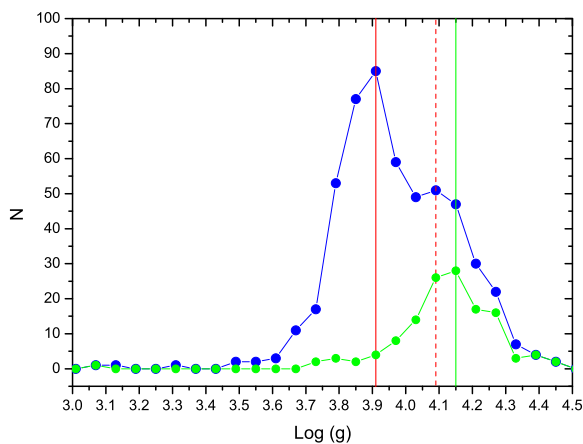


Figure 6. Distribution of the gravitational acceleration $\log g$. The solid and the dashed lines represent to the two peaks near 3.91 and 4.09, respectively. The green line refers to the peak for UCVs. Symbols are the same as those in Fig. 5.

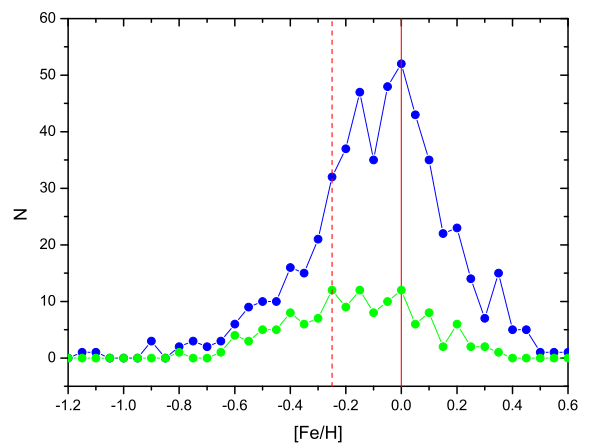


Figure 7. Distribution of the metallicity [Fe/H] for δ Scuti variables observed by LAMOST. It is shown that most of the δ Scuti stars have metallicity close to the Sun, i.e., [Fe/H] \sim 0 (the solid line), while the metallicity of most UCVs are mainly from about -0.25 (the dashed line) to 0.0. Symbols are the same as those in Figs 5 and 6.

Table 5. 50 δ Scuti pulsating stars with the difference of radial velocity larger than 15 km s^{-1} .

Name	Period (d)	Dates	Times	T (K)	$\log g$	[Fe/H]	V_{Low}	V_{High}	ΔV
KIC 5722346	0.0883	2013-10-05–2015-10-08	3	7130	3.90	0.45	-53	11	64
ASAS J081813-0049.8	0.139603	2013-11-25–2015-02-05	2	7129	3.80	0.21	-47	11	58
KIC 10014548	0.65445	2012-06-04–2017-06-14	11	7206	3.83	0.56	-102	-50	52
ASAS J085536+0215.5	0.207902	2012-02-10–2016-04-03	3	5970	4.30	-0.36	-25	18	43
ASAS J022414+2741.6	0.155998	2013-10-06–2017-01-28	2	5713	4.26	-0.05	-85	-44.45	40.55
ASAS J154613-0026.1	0.068991	2012-05-16–2016-05-18	3	7458	4.05	-0.37	-10	27	37
NSVS 11000901	0.39787221	2017-04-22–2017-06-11	2	6899	4.10	-0.20	-49.3	-13.65	35.65
KIC 4252757	0.046555	2012-06-15–2014-06-02	2	7541	3.95	-0.09	-68	-34	34
KIC 7350486	0.75188	2013-09-26–2017-06-15	4	7127	3.89	0.10	-59	-25	34
KIC 3634384	0.085852	2012-06-15–2014-06-02	3	7360	3.87	0.10	-5	27	32
BS Cnc	0.051	2015-03-08–2016-02-24	4	7471	3.89	0.07	5	36	31
KIC 5476864	0.59988	2013-10-05–2014-05-22	2	7068	4.08	0.09	-38	-9	29
KID 4252716	0.076184	2012-06-15–2017-06-03	2	7505	3.86	-0.06	-40	-11.89	28.11
KIC 3942911	0.03391	2012-06-15–2015-10-12	6	7438	3.96	0.05	-39	-11	28
ASAS J125114+0917.7	0.182872	2014-01-13–2017-05-17	2	5795	4.18	0.03	-14	13.9	27.9
NSVS 3820963	0.16784703	2014-11-04–2015-12-28	2	5660	4.26	-0.13	-98	-71	27
BD+24 95	0.11992	2012-09-29–2013-12-19	4	7092	3.75	0.49	-33	-7	26
KIC 9391395	0.51308	2014-05-02–2017-06-15	7	7236	4.05	-0.19	-30	-4	26
KIC 11193046	0.78431	2013-05-22–2017-05-16	3	7993	3.92	-0.12	-25	0.6	25.6
KIC 8429756	0.036041	2013-05-19–2015-10-11	2	7457	3.85	-0.06	-31	-6	25
LINEAR 9272851	0.080104	2016-01-13–2016-02-06	2	7192	4.26	-0.88	249	273	24
ASAS J075428+1407.8	0.189175	2013-02-15–2013-12-14	3	6073	4.29	-0.41	29	53	24
ASAS J113810+1905.1	0.153786	2015-12-21–2017-05-15	2	5806	3.97	-0.21	-35.13	-12	23.13
V0367 Cam	0.121596	2012-01-13–2016-01-19	4	7307	3.84	0.26	-16	7	23
KIC 5768203	0.12807	2013-10-07–2017-06-07	2	6962	4.28	-0.59	-33	-10.27	22.73
KIC 9072011	0.16351	2014-05-29–2017-05-14	2	7026	3.69	0.23	-34	-13.08	20.92
NSV 19942	0.16352	2015-01-23–2017-06-07	3	7099	3.72	0.45	-2	18.27	20.27
KIC 3119604	0.024301	2012-06-15–2017-06-13	2	7940	4.20	-0.26	-50	-30.42	19.58
KIC 9450940	0.033337	2014-05-29–2015-10-06	3	7922	4.08	-0.20	-61	-42	19
KIC 7106205	0.074655	2013-05-19–2017-06-15	10	7173	3.86	0.13	-29	-10	19
ASAS J064626+2629.8	0.205972	2012-03-11–2016-01-18	4	6613	4.19	-0.25	0	19	19
ASAS J083952+0052.4	0.133043	2013-03-24–2013-03-24	2	4660	4.37	0.03	51	70	19
KID 6593488	0.10101	2015-09-25–2016-05-18	3	7026	3.96	-0.09	-42	-24	18
BD+38 2361	0.049839	2014-01-12–2016-01-28	2	7411	3.97	-0.08	-34	-16	18
KIC 8460993	0.05535	2013-09-25–2017-06-14	3	7193	3.90	0.25	-68	-50	18
KIC 9700679	3.81679	2013-10-04–2017-06-15	5	5491	3.17	0.10	-23	-5.06	17.94
KIC 9473000	0.11496	2012-06-04–2017-05-16	2	7376	3.99	0.04	-31.03	-14	17.03
GSC 01946-00035	0.06708077	2013-12-01–2014-12-02	4	7267	4.00	-0.03	59	76	17
ASAS J190751+4629.2	0.079561	2013-10-04–2015-05-30	4	7174	3.91	0.19	-71	-54	17
NSVS 9420734	0.19695349	2014-09-17–2016-02-10	3	6015	3.97	0.04	-20	-3	17
ASAS J163007+0125.2	0.160533	2013-03-24–2013-03-24	2	5542	4.26	-0.26	-33	-16	17
KIC 5272673	0.059492	2012-06-17–2017-06-13	3	7156	3.95	0.38	-45	-28.26	16.74
KID 2304168	0.123344	2012-06-15–2017-06-13	2	7222	3.86	0.09	-32	-15.42	16.58
HAT 199-00623	0.29481	2012-06-17–2015-10-18	2	6930	3.49	0.42	-75	-59	16
KIC 9052363	0.023829	2013-09-25–2015-10-03	3	7840	4.08	-0.15	-32	-16	16
KIC 9156808	0.046995	2014-09-13–2017-06-14	3	7139	4.11	-0.03	-26	-10.56	15.44
ASAS J093944+0010.3	0.196522	2012-02-16–2015-01-03	2	6170	4.15	-0.22	29	44	15
NSVS 9431318	0.17746757	2013-02-09–2014-11-01	3	6089	4.08	-0.56	49	64	15
1SWASP J032748.43+343810.3	0.11771	2013-09-14–2014-11-01	2	7166	3.95	-0.25	-30	-15	15
KIC 7977996	0.090662	2013-10-05–2015-10-08	2	7318	4.14	-0.11	2	17	15

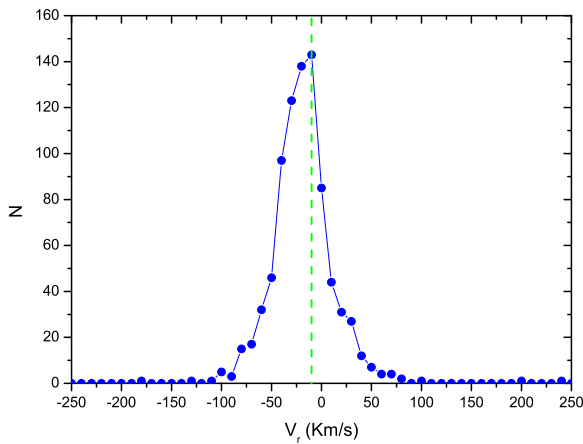
525 δ Scuti stars observed by LAMOST is shown in Fig. 5 as blue dots. As displayed in the figure, there are two peaks in the distribution. The main peak is at 7150 K, while the other small peak is near 5950 K. Also shown in the figure as green dots is the temperature distribution for the 131 UCVs. It suggests that the small peak is caused by the existence of the UCVs indicating that they are solar-type cool stars.

The distribution of the gravitational acceleration $\log g$ is plotted in Fig. 6. The main peak of the distribution is near 3.91. Apart from the main peak, there is a small peak at 4.09. These properties reveal that δ Scuti variable stars populate on the instability strip

slightly above the zero-age main sequence (ZAMS), the main sequence, and the early stages of H-shell burning. The green dots in the figure represent the distribution of the gravitational acceleration $\log g$ for UCVs where the peak is at 4.15 indicating that their gravitational accelerations are higher than the others. The metallicity ([Fe/H]) distribution is shown in Fig. 7. The peak of the distribution is near [Fe/H] \sim 0 indicating that most of the δ Scuti variables have metallicity close to that of the Sun. 10 δ Scuti stars have the highest metallicities are shown in Table 4. As those in Figs 5 and 6, the green dots in Fig. 7 refer to the distribution for UCVs. It is

Table 6. 38 δ Scuti variable stars with radial velocities higher than 70 km s^{-1} .

Name	Period (d)	Sp.	T (K)	$\log g$	[Fe/H]	V_r (km s^{-1})
LINEAR 9272851	0.080104	A7V	7060	4.23	-0.94	273
KID 8004558	0.042706	A5V	7450	4.29	-0.89	-262
LINEAR 9272851	0.080104	A7V	7220	4.27	-0.87	249
LINEAR 23008936	0.060405	A5V	7320	4.24	-0.74	200
LINEAR 565638	0.086365	A7IV	6750	4.23	-0.74	-177
LINEAR 19119847	0.080278	A7V	7330	4.16	-0.27	-122
KIC 10014548	0.65445	F0	7230	3.74	0.58	-102
LINEAR 3753972	0.064807	A6IV	7511	4.29	-0.72	101.18
Renson 31680	0.46666	A7V	7570	4.12	-0.36	-99
NSVS 3820963	0.167847	G4	5740	4.29	-0.12	-98
KIC 10014548	0.65445	F0	7230	3.84	0.57	-96
Renson 31680	0.46666	A7V	7540	4.10	-0.37	-95
Renson 31680	0.46666	A7V	7480	4.12	-0.36	-94
ASAS J053125+1103.8	0.144799	F2	5970	4.23	-0.33	88
CR Ari	0.18094	A2V	7110	3.92	-0.79	-87
ASAS J022414+2741.6	0.155998	G3	5690	4.23	-0.06	-85
ASAS J152257+1054.4	0.054955	A5V	8280	4.07	-0.31	-83
ASAS J053125+1103.8	0.144799	F8	5860	4.08	-0.43	82
ASAS J170044-0241.3	0.160861	G2	5750	3.99	-0.26	-80
ASAS J135248+1150.2	0.186274	F5	6340	4.23	-0.47	-79
ASAS J151411+2043.1	0.212255	G4	5660	4.09	0.04	-79
V0460 And	0.074981	A6IV	8120	4.16	-0.25	-77
ASAS J084602+1301.4	0.121261	F0	7340	3.93	0.12	77
KIC 10014548	0.65445	F0	7230	3.82	0.59	-77
GSC 01946-00035	0.067081	F0	7210	3.98	0.01	76
HAT 199-00623	0.29481	F0	7030	3.59	0.43	-75
CSS_J085942.7+190007	0.180998	F2	6160	4.30	-0.49	-75
KIC 5038228	1.10619	F0	7250	3.62	0.45	-74
GSC 01732-00480	0.0606	A7V	7701	4.16	-0.38	-72.77
V1116 Her	0.094683	A7V	7750	4.12	-0.41	-72
ASAS J084602+1301.4	0.121261	F0	7570	3.92	0.08	72
VSX J175138.3+373909	0.04038	A7V	7570	3.86	0.11	-72
ASAS J155047+0505.4	0.15218	G3	5730	4.19	-0.18	-71
ASAS J190751+4629.2	0.079561	F0	7190	3.93	0.17	-71
NSVS 3820963	0.167847	G3	5660	4.26	-0.13	-71
Galati V3	0.098	F0	7190	3.96	0.06	-71
ASAS J083952+0052.4	0.133043	K5	4550	4.36	0.04	70
ASAS J180757+0901.8	0.10531	A6IV	7270	3.96	0.02	-70

**Figure 8.** Distribution of the radial velocity V_r for δ Scuti pulsating stars observed by LAMOST. There is a peak near $V_r = -10 \text{ km s}^{-1}$.

shown that most UCVs have Fe/H from about -0.25 to 0.0 revealing that they are slightly metal poor than the normal δ Scuti stars.

The distribution of the radial velocity (V_r) for those δ Scuti variable stars is displayed in Fig. 8. 843 RVs for 525 δ Scuti variable stars were determined by LAMOST from 2011 October 24 to 2017 June 16 and they are used for constructing the figure. A peak is near $V_r = -10 \text{ km s}^{-1}$ indicating that the V_0 of most variable stars are close to this value. The relation between the pulsating period and the radial velocity is displayed in Fig. 9 where the dashed line refers to the distribution peak of the radial velocity. Those radial velocities of δ Scuti stars are useful to investigate their binarities. It is known that about 60%–80% of field stars in the solar neighbourhood are members of binary or multiple systems (e.g., Duquenoey Mayor 1991). A very interesting question is how much percent for δ Scuti stars are in binaries or multiples? Gravitational effects of close binary companions may be important to influence the non-radial pulsations through tidal interactions (e.g., Szatmary 1990). In the catalogue published by Rodríguez et al. (2000), 86 δ Scuti stars were pointed out as members of binary or multiple systems. Among 1578 δ Scuti stars in the most recent catalogue published by Chang et al. (2013), 141 cases belong to binaries or multiples.

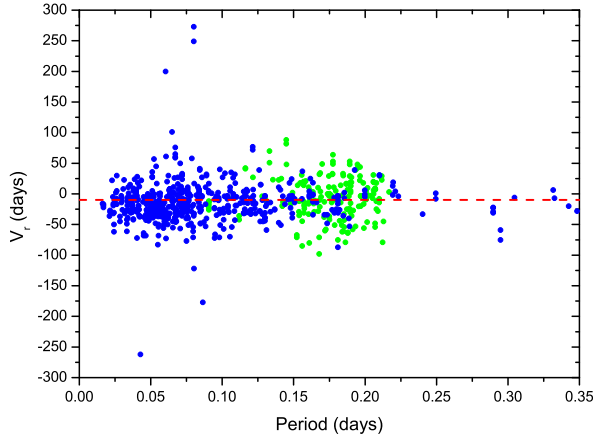


Figure 9. The correlation between the radial velocity and the pulsating period. Blue dots refer to NDSTs, while green dots to UCVs (see text for details). The red dashed line represents the peak of the distribution peak of the radial velocity.

Some of the binary δ Scuti systems were detected by analysing the light-travel time effect (e.g., Li et al. 2010, 2013; Qian et al. 2015).

Among binary δ Scuti systems, there is an interesting group of eclipsing binaries that are commonly referred to as *q̄oEA stars* (i.e., oscillating eclipsing systems of Algol type). They are a new class of stellar systems where (B)A-F type primaries are the mass-accreting δ Scuti stars (e.g., Mkrtichian et al. 2002; Liakos et al. 2012). Physical properties of those binary δ Scuti stars were investigated by some investigated (e.g., Mkrtichian et al. 2003; Soyugan et al. 2006; Liakos & Niarchos 2017; Kahraman et al. 2017). Because of the pulsation, the radial-velocity changes should be associated with the light variations of δ Scuti stars. However, the information on the radial velocity extremely lacks.

Among the 525 δ Scuti pulsating stars derived spectroscopic parameters, 178 were observed two times or more by LAMOST. The difference between the lowest and the highest radial velocities are determined. 50 δ Scuti stars with V_r difference larger than 15 km s^{-1} are listed in Table 5. The peak-to-peak radial-velocity amplitude for δ Scuti stars is usually in the range from 5 to 10 km s^{-1} (e.g., Breger et al. 1976; Yang & Walker 1986). In previous section, the LAMOST data have been compared with those determined by using high-resolution optical spectra collected from the literature by Frasca et al. (2016). It is shown that the standard deviation for radial velocity V_r is 11 km s^{-1} . There those δ Scuti stars with $\Delta V_r > 15 \text{ km s}^{-1}$ may be the candidates of binary or multiple systems. Moreover, as shown in Fig. 9, the radial velocities for most δ Scuti stars are around $V_r = -10 \text{ km s}^{-1}$. However, the radial velocities of some δ Scuti variables are very high. 38 δ Scuti stars with $V_r > 70 \text{ km s}^{-1}$ are shown in Table 6. They are also candidates of binary δ Scuti systems.

4 SEVERAL STATISTICAL CORRELATIONS FOR NORMAL δ SCUTI STARS

In this section, we analyze the relationships between the pulsating period and those stellar atmospheric parameters (e.g., temperature, gravitational acceleration, and metallicity) and then inves-

tigate physical properties of the δ Scuti stars. Since the UCVs are quite different from the normal ones. When we investigate the physical properties of NDSTs, they should be excluded. As shown in Fig. 4, there is a good relation between the pulsating period (P) and the effective temperature (T) for NDSTs. A least-squares solution yields,

$$T = 7233.5(\pm 36.7) + 1251.3(\pm 242.0) \exp\left[-\frac{P}{0.033(\pm 0.007)}\right]. \quad (1)$$

This relation (the solid red line) shows that the hotter δ Scuti stars tend to have extremely shorter periods than the late-type variables. It can be explained as an evolutionary effect because the hotter δ Scuti stars tend to be near the main sequence, while cooler variables are more evolved (e.g., Rodríguez et al. 2000).

The correlation between the period and the gravitational acceleration $\log g$ is shown in Fig. 10 where 10 δ Scuti variable stars without period in VSX are not displayed. Their atmosphere parameters are listed in Table 7. Blue dots in the figure refer to NDSTs, while the green ones to UCVs. The two dashed lines are the borders of UCVs. It is well known that there is a basic relation for pulsating stars,

$$P \sqrt{\rho/\rho_{\odot}} = Q, \quad (2)$$

where ρ is the mean density, Q is the pulsation constant. As stars evolving from zero-age main sequence, both the the mean density ρ and the gravitational acceleration $\log g$ should be decreasing. Therefore, the pulsating period should be increasing according to equation (2). It is expected that there is a well correlation between the pulsating period and the gravitational acceleration, i.e., the long-period δ Scuti stars have low gravitational accelerations. As shown in Fig. 10, no such relation can be seen if all sample stars are considered. However, after UCVs are excluded, a well relation (the solid red line) between the period and the gravitational acceleration is detected for NDSTs with period shorter than 0.3 d. A least-squares solution leads to the follow equation,

$$\log g = 4.046(\pm 0.015) - 1.168(\pm 0.152) \times P. \quad (3)$$

This relation is a strong observational evidence for the theoretically basic relation for pulsating stars.

The relation between the pulsating period and the metallicity $[\text{Fe}/\text{H}]$ for short-period δ Scuti stars is plotted in Fig. 11. For comparison, those UCVs are also shown in the figure as green dots. For SX Phe-type pulsating stars in the globular clusters, there is a correlation between the metallicities and the periods of the variables (e.g., McNamara 1995, 1997; Rodríguez & Breger 2000). As shown in Fig. 11, the metallicity is weakly correlated with the period (the solid red line). By using the least-squares method, the following equation,

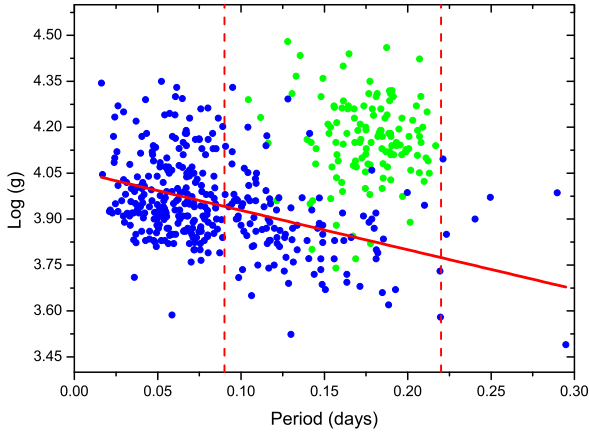
$$[\text{Fe}/\text{H}] = -0.121(\pm 0.026) + 0.92(\pm 0.25) \times P, \quad (4)$$

is derived after UCVs are excluded. The relation tell us that metal-poor stars enter the instability strip mostly with periods shorter than 0.1 d. By using equation (4), we could obtain $[\text{Fe}/\text{H}]=0$, when $P=0.132 \text{ d}$. This indicating that a δ Scuti star with a solar metallicity should has a typical period of $P=0.132 \text{ d}$. This statistical relation could be explained as that metal-poor pulsating stars evolving into pulsationally unstable states from main sequences displaced below the metal-strong main sequence (e.g., McNamara 1997).

Among the δ Scuti stars catalogued by Chang et al. (2013), 83 of them were observed by LAMOST including 33 UCVs and 50 NDSTs. By using the photometric data in the V-band collected by Chang et al. (2013), the correlation between the period and the

Table 7. LAMOST observations of δ Scuti variable stars without periods listed in VSX.

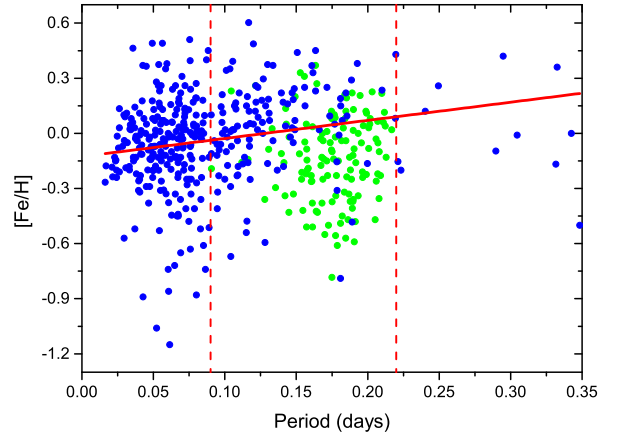
Name	$\alpha(2000)$	$\delta(2000)$	Dates	Sp.	T (K)	$\log g$	[Fe/H]	V_r (km s $^{-1}$)
GP Cnc	129.5405	7.22583	2015-02-06	F0	7320	4.12	-0.39	-11
V0501 Per	63.96912	51.21828	2012-02-08	F0	7140	4.26	-0.14	-13
UV Tri	23.00046	30.36569	2013-10-04	F0	7250	3.89	0.14	25
NSV 1273	56.39346	24.46328	2016-11-10	A6IV	7317	4.11	-0.08	1.57
NSV 1273	56.39346	24.46328	2016-09-30	A6IV	7294	4.08	-0.10	2.94
[EHV2002]1-5-0832	91.85333	45.9975	2013-12-15	F0	6980	4.11	-0.39	-41
HD 12899	31.67329	14.58378	2012-09-30	F0	7170	3.85	0.06	-15
HD 89503	154.9601	7.61394	2016-01-22	F0	7540	3.79	-0.08	1
HD 89503	154.9601	7.61394	2015-04-24	A7V	7450	3.87	-0.03	-5
BD+19 572	55.00588	19.81067	2016-01-29	K1	5070	2.84	0.05	17
BD+16 1693	125.09	15.86461	2016-03-13	F0	7130	3.82	0.10	12
HD 221012	352.119	18.69408	2014-11-05	A7V	7610	4.01	0.00	0

**Figure 10.** The relation between the pulsating period and the gravitational acceleration for short-period NDSTs ($P < 0.3$ d). Blue dots refer of NDSTs, while green ones to UCVs that are between the two red dashed line. The red solid line represents the linear relation between the period and the gravitational acceleration.

photometric amplitude is displayed in Fig. 12 where blue dots refer of NDSTs, while green ones to UCVs. Apart from the variables observed by LAMOST, the other targets investigated by Chang et al. (2013) are also shown as magenta dots. As pointed out by Chang et al. (2013), the amplitudes are usually in the range of 0.003-0.9 mag in the V band and this figure tells us that there is no relation between amplitudes and periods for the field stars. Rodríguez & Breger (2001) mentioned that pulsating variables in the period range from 0.25 to 0.3 d may need to be reclassified as evolved Population I δ Scuti or Population II RRc (or γ Dor). As can be seen in Fig. 12, the amplitudes of UCVs are similar to those of NDSTs. The UCVs are solar-type cool variables that have periods in the range from 0.09 to 0.22 d (the two dashed red lines). There are many δ Scuti stars whose pulsating periods are in the period range. It is possible that some of them belong to UCVs and they need to be reclassified.

5 DISCUSSIONS AND CONCLUSIONS

In the past 20 years, the number of δ Scuti variable stars is enormously increasing. In addition to the immense effort developed by

**Figure 11.** The relation between the pulsating period and the metallicity [Fe/H] for short-period δ Scuti variable stars. Symbols are the same as those in Fig. 10. It is shown that there is a linear correlation between the pulsating period and the metallicity.

several photometric surveys on the ground, several space missions such as MOST (Walker et al. 2003), CoRoT (Baglin et al. 2006) and Kepler (Borucki et al. 2010) were carried out that led to the discovery of a lot of new variables and provide high-precision photometry. However, spectroscopic information for those Scuti stars are lack. Among 3689 δ Scuti variables listed in VSX catalogue, 766 of them were observed in LAMOST spectral survey from 2011 October 24 to 2017 June 16. We catalogue those δ Scuti stars and their spectral types are given. Stellar atmospheric parameters for 525 ones are presented. By analysing 32 δ Scuti variables observed four times or more, we show that the standard errors of the effective temperatures, the gravitational acceleration and the metallicity are usually lower than 100 K, 0.1 dex and 0.08 dex, respectively. The atmospheric parameters for 352 stars were determined by Frasca et al. (2016) who mainly used high-resolution optical spectra collected from the literature. To check the LAMOST data (DR4 and the first three quarters of DR5) released recently, their LAMP data are compared with those derived by Frasca et al. (2016). It is shown in Fig. 2 that there are very good agreements for the four stellar atmospheric parameters. The determined standard deviations are 135 K for T , 0.21 dex for $\log g$, 0.14 dex for [Fe/H], and 11 km/s

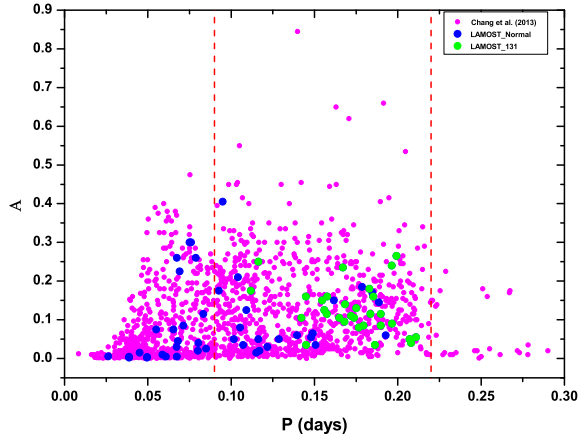


Figure 12. The relation between the period and the photometric amplitude (A) for NDSTs and UCVs. Those V-band photometric amplitudes were from Chang et al. (2013). Blue dots refer of NDSTs, while green ones to UCVs. For comparison, the other targets are also shown as magenta dots.

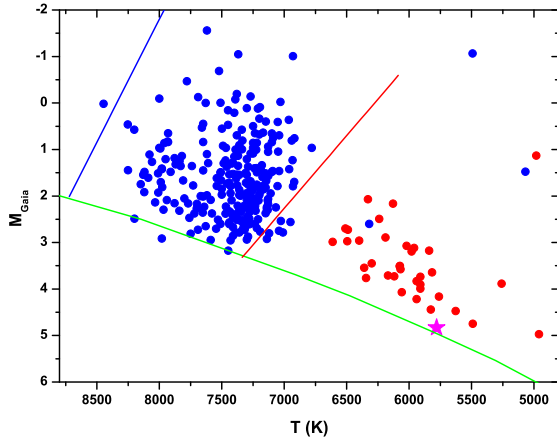


Figure 13. The $H-R$ diagram for δ Scuti variable stars observed by both LAMOST and *GAIA*. Blue dots refer to NDSTs, while red dots to UCV ones. The position of the Sun is plotted as the red star. The solid blue line and the red dashed line represent the blue and red edges of δ Scuti variables from McNamara (2000). The green line stands for zero-age main sequence from Kippenhahn et al. (2012).

for V_r , respectively. Meanwhile, the LASP data of the 188 δ Scuti stars in the LAMOST-Kepler field are also compared with those derived by using the ROTFIT code (Frasca et al. 2016). The results indicate that stellar atmospheric parameters for those δ Scuti stars derived by LAMOST are reliable.

As shown in Table 5, 50 δ Scuti stars have radial velocity differences larger than 15 km s^{-1} among 178 δ Scuti stars that were observed two times or more by LAMOST. They may be candidates of binary δ Scuti systems. Moreover, the radial velocities of some δ Scuti variables are very high. Table 6 shows that 38 δ Scuti variables have radial velocities higher than $V_r = 70 \text{ km s}^{-1}$. They may

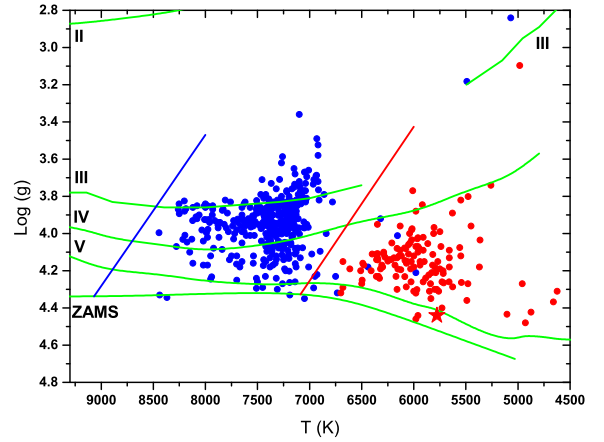


Figure 14. The $\log g - T$ diagram for δ Scuti variable stars observed by LAMOST. Symbols are the same as those in Fig 12. The blue and red lines represent the blue and red edges of δ Scuti instability strip from Rodríguez & Breger (2001). The green lines stand for the luminosity classes range between II and V that are from Straizys & Kuriliene (1981), while the zero-age main-sequence line is from Cox (2000).

be also the members of binary or multiple systems. Some of those δ Scuti systems may be eclipsing binaries with high orbital inclinations. If they are real binary systems, the change of the relative distance of the δ Scuti variables from the Sun can result in the observed cyclic change in the O-C (the Observed-Computed maxima times) diagram when the δ Scuti stars orbit the barycenter of the binary system. Therefore, they could be confirmed by monitoring their maxima through the analyses of the light-travel time effect (e.g., Li et al. 2010, 2013; Qian et al. 2015).

By analysing stellar atmospheric parameters of δ Scuti pulsating stars derived by LAMOST, we show that there is a group of 131 UCVs with period in the range from 0.09 to 0.22 d. The UCVs are solar-type stars with temperature lower than 6700 K. It is found that there are two peaks on the distributions of the period, the effective temperature, the gravitational acceleration, and the the metallicity. One is the main peak, while the other is a small one. We show that the small peaks in those distributions are mainly caused by the existence of this group of variable stars. Those UCVs are more metal poor stars and have higher gravitational accelerations than those of NDSTs.

Among the 525 δ Scuti pulsating stars whose stellar atmospheric parameters were determined by LAMOST, 297 were also observed by *Gaia* (Prusti et al. 2016) including 262 NDSTs and 35 UCVs. Their parallaxes and apparent magnitudes were given in *Gaia* Data Release 1 (Brown et al. 2016). The $H-R$ diagram of the δ Scuti stars observed by both LAMOST and *Gaia* is plotted in Fig. 13 where the effective temperature are from LAMOST, while the photometric absolute magnitudes are determined by using *Gaia* data. The the blue and red edges for δ Scuti stars are from McNamara (2000). The green line in the figure represents the zero-age main sequence from Kippenhahn et al. 2012. As shown in the figure, apart from three targets, KIC 9700679 ($P = 3.81679 \text{ d}$), TAOS 59.00115 ($P = 0.038706 \text{ d}$), and $BD + 19^\circ 572$ (without period), the rest NDSTs locate inside the classical Cepheid instability

strip, while the UCVs are far beyond the red edge of instability strip. It is shown that those UCVs are more evolved than the Sun.

The relations between the gravitational acceleration ($\log g$) and the effective temperature (T) for all variable stars observed by LAMOST is shown in Fig. 14 where blue dots refer to NDSTs, while red dots to UCVs. The position of the Sun is plotted as the red star. The blue and red lines in the figure stand for the borders of δ Scuti pulsating stars. Those green lines shown represent stellar luminosity classes range between II and V that are from Straizys & Kurilienne (1981), while the zero-age main-sequence line is from Cox (2000). As that shown in the H-R diagram, it is found that all of the UCVs are beyond the red edge of δ Scuti instability strip. Most of them are evolved from zero-age main-sequence stars with luminosity classes range between IV and V. One UCV, KIC 8747415, may be giant or sub-giant with $\log g = 3.097$. There are several targets, e.g., KIC 9700679 ($P = 3.81679$ d), KIC 5446068 ($P = 3.48432$ d), BOKS-24178 ($P = 0.7$ d), ASAS J070907+2656.7 ($P = 0.043322$ d), TAOS 59.00115 ($P = 0.038706$ d), and *BD + 19°572* (without period), are beyond the red edge of δ Scuti stars with temperatures below 6700 K. Their periods are not in the range between 0.09 and 0.22 days. Although they were classified as NDSTs, their physical properties are special and need to be investigated in the future. As shown in Figs 13 and 14, there is a gap between zero-age main sequence and the position of NDSTs in the H-R diagram and in the $\log g - T$ diagram. The gaps increase with growing effective temperature (e.g., Balona & Dziembowski 2011).

Those UCVs should be excluded when we investigate the physical properties of NDSTs because they are quite different from the others. It is found that there is a good relation between the effective temperature (T) and the pulsating period (P) for NDSTs. It shows that the temperature is rapidly decreasing when the period is increasing. This relation reveals that the hotter δ Scuti stars tend to be near the main sequence while cooler variables are more evolved (e.g., Rodríguez et al. 2000). A well relation between the gravitational acceleration and the period is discovered for short-period δ Scuti stars with period shorter than 0.3 d (solid red line in Fig. 10). The gravitational acceleration is decreasing as the period increasing. This relation is a direct observational evidence for the theoretically basic relation in equation (3) for pulsating stars. Moreover, the metallicity is detected to be weakly correlated with the period as that found for SX Phe-type pulsating stars in the globular clusters (e.g., McNamara 1997).

To check whether those UCVs are δ Scuti stars or not, their pulsation constants (Q) are calculated by using the following equation given by Breger (1990),

$$\log(Q/P) = 0.5 \log g + 0.1 M_{bol} + \log T - 6.456. \quad (5)$$

The effective temperature T and the gravitational acceleration $\log g$ are from the data of LAMOST, while M_{bol} could be computed with the equation (e.g., McNamara 2011),

$$M_{bol} = -2.89 \log P - 1.31. \quad (6)$$

The results are shown in Fig. 15, where the dashed red line refers to $Q = 0.033$ d. As displayed in the figure, the values of Q for most of UCVs are larger than 0.033 days. As δ Scuti stars are p-mode and mixed-mode pulsators, Q needs to be below 0.033 d (e.g., Fitch 1981). Therefore, the derived results may indicate that most UCVs do not belong to δ Scuti pulsating stars. The other method to check them is to determine the ratios of radial velocity to light amplitude of the stellar variability. If they are δ Scuti pulsating stars, the ratios should be in the range from 40 to 120 $\text{km}^{-1} \text{mag}^{-1}$ (e.g., Breger

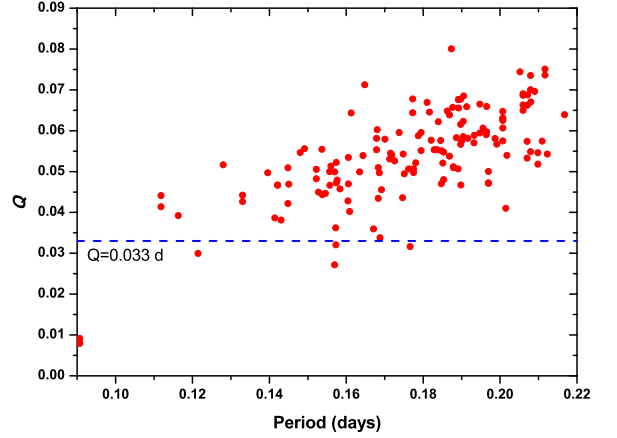


Figure 15. The plot of the pulsation constant (Q) along with the period for the UCVs observed by LAMOST. The dashed red line refers to $Q = 0.033$ d. It is shown the values of Q for most of UCVs are larger than 0.033 d indicating that they may not be δ Scuti pulsating stars.

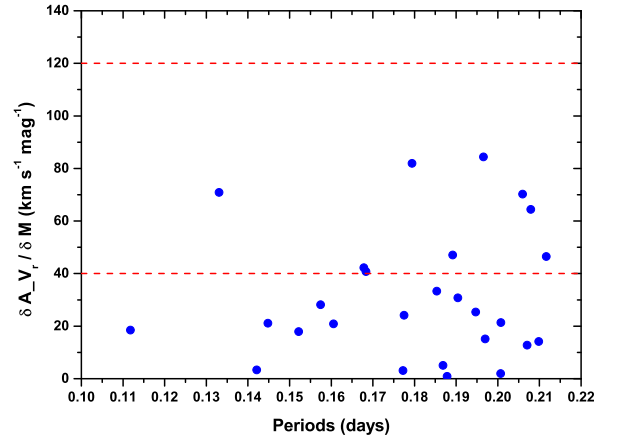


Figure 16. A plot of the ratio of radial velocity to light amplitude along with the period for 28 UCVs observed two times or more. The two red dashed lines refer to the range for δ Scuti stars.

et al. 1976; Daszynska-Daszkiewicz et al. 2005). 28 UCVs were observed two times or more and the difference between the lowest and the highest radial velocities are determined. Then the ratios of radial velocity to light amplitude could be estimated and the results are plotted in Fig. 16. As shown in the figure, although some ratios are below 40 $\text{km}^{-1} \text{mag}^{-1}$, we could not rule out them as δ Scuti stars because our data are insufficient to derive the amplitude of the radial velocity curve.

Some UCVs are classified as both δ Scuti stars (DSCT) and EC-type contact binaries implying that they are actually suspected as contact binaries, i.e. their variability classification is not unique. Those suspected contact binary stars may have double periods, i.e., in the period range from 0.18 to 0.44 d. This is typical range for EW-type contact binary systems (see fig. 1 in Qian et al. 2017a).

Those binary stars are similar to contact systems investigated by Qian et al. (2007, 2013, 2014). Moreover, as listed in Table 7, several UCVs show large radial velocity scatters indicating that they may be close binary stars. In this way, the derived effective temperatures for those sample stars are very useful during solving their light curves. The other atmospheric parameters (e.g., $\log g$ and $[\text{Fe}/\text{H}]$) will provide us valuable information to understand their formation and evolutionary state. Our results show that about 25% of the known δ Scuti pulsating stars may be misclassified. They may be close binary stars rather than δ Scuti stars. As shown in Fig. 1, about 1800 objects listed in VSX are classified as δ Scuti pulsating stars in the period range from 0.09 to 0.22 d. Some of them may need to be reclassified.

The blue edge of the instability strip for δ Scuti stars is theoretically well constrained (e.g., Pamyatnykh 2000). However, the red edge is rather complicated and has a large range of possibilities for the slope and shape (e.g., Chang et al. 2013). The investigation of some authors (e.g., Houdek et al. 1999) indicated that oscillations in solar-like stars are intrinsically damped and stochastically driven by convection, while the calculations by Cheng & Xiong (1997) using the theory of Xiong (1989) predicted over stable solar oscillations. If some UCVs are confirmed as pulsating stars, they may be a new-type pulsator. Their observations and investigations will shed light on theoretical instability domains and on the theories of interacting between the pulsation and the convection of solar-type stars. New observations and detailed investigations on UCVs are timely and required urgently in the near future.

ACKNOWLEDGEMENTS

This work is partly supported by National Natural Science Foundation of China (No. 11325315). Guoshoujing Telescope (the Large Sky Area Multi-Object Fiber Spectroscopic Telescope LAMOST) is a National Major Scientific Project built by the Chinese Academy of Sciences. Funding for the project has been provided by the National Development and Reform Commission. LAMOST is operated and managed by the National Astronomical Observatories, Chinese Academy of Sciences. Spectroscopic observations used in the paper were obtained with LAMOST from 2011 October 24 to 2016 November 30. This work has made use of data from the European Space Agency (ESA) mission *Gaia* (<https://www.cosmos.esa.int/gaia>), processed by the *Gaia* Data Processing and Analysis Consortium (DPAC; <https://www.cosmos.esa.int/web/gaia/dpac/consortium>). Funding for the DPAC has been provided by national institutions, in particular the institutions participating in the *Gaia* Multilateral Agreement.

REFERENCES

- Baglin, A., Auvergne, M., Barge, P., et al. 2006, The CoRoT Mission Pre-Launch Status - Stellar Seismology and Planet Finding, 1306, 33
- Balona, L. A., & Dziembowski, W. A. 2011, MNRAS, 417, 591
- Borucki, W. J., Koch, D., Basri, G., et al. 2010, Science, 327, 977
- Breger, M. 1979, PASP, 91, 5
- Breger, M. 1990, Delta Scuti Star Newsletter, 2, 13
- Breger, M. 2000, Delta Scuti and Related Stars, 210, 3
- Breger, M., Hutchins, J., & Kuhl, L. V. 1976, ApJ, 210, 163
- Breger, M., Lenz, P., Antoci, V., et al. 2005, A&A, 435, 955
- Brown, A. G. A., Vallenari, A., et al. 2016, A&A, 595, A2
- Chang, S.-W., Protopapas, P., Kim, D.-W., & Byun, Y.-I. 2013, AJ, 145, 132
- Cheng, Q. L., & Xiong, D. R. 1997, A&A, 319, 981
- Cox, A. N. 2000, Allen's Astrophysical Quantities, 4th ed. (New York: Springer), P.381
- Cui, X.-Q., Zhao, Y.-H., Chu, Y.-Q., et al. 2012, Research in Astronomy and Astrophysics, 12, 1197
- Daszyńska-Daszkiewicz, J., Dziembowski, W. A., Pamyatnykh, A. A., et al. 2005, A&A, 438, 653
- Duquenooy, A., & Mayor, M. 1991, A&A, 248, 485
- Fitch, W. S. 1981, ApJ, 249, 218
- Prusti, T., de Bruijne, J. H. J., et al. 2016, A&A, 595, A1
- Gao, H., Zhang, H.-W., Xiang, M.-S., et al. 2015, Research in Astronomy and Astrophysics, 15, 2204
- Gautschi, A., & Saio, H. 1995, ARA&A, 33, 75
- Houdek, G., Balmforth, N. J., Christensen-Dalsgaard, J., & Gough, D. O. 1999, A&A, 351, 582
- Gray, R. O., Corbally, C. J., De Cat, P., et al. 2016, AJ, 151, 13
- Kahraman Aliçavuş, F., Soyduğan, E., Smalley, B., & Kubát, J. 2017, MNRAS, 470, 915
- Frasca, A., Alcalá, J. M., Covino, E., et al. 2003, A&A, 405, 149
- Frasca, A., Guillout, P., Marilli, E., et al. 2006, A&A, 454, 301
- Frasca, A., Molenda-Żakowicz, J., De Cat, P., et al. 2016, A&A, 594, A39
- Kippenhahn, R., Weigert, A., & Weiss, A. 2012, Stellar Structure and Evolution: , Astronomy and Astrophysics Library. ISBN 978-3-642-30255-8. Springer-Verlag Berlin Heidelberg
- Koleva, M., Prugniel, P., Bouchard, A., & Wu, Y. 2009, A&A, 501, 1269
- Lopez de Coca, P., Rolland, A., Rodriguez, E., & Garrido, R. 1990, A&AS, 83, 51
- Li, L.-J., Qian, S.-B., & Xiang, F.-Y. 2010, PASJ, 62, 987
- Li, L.-J., & Qian, S.-B. 2013, PASJ, 65, 116
- Liakos, A., & Niarchos, P. 2017, MNRAS, 465, 1181
- Liakos, A., Niarchos, P., Soyduğan, E., & Zsche, P. 2012, MNRAS, 422, 1250
- Luo, A.-L., Zhao, Y.-H., Zhao, G., et al. 2015, Research in Astronomy and Astrophysics, 15, 1095
- McNamara, D. H. 1995, AJ, 109, 1751
- McNamara, D. 1997, PASP, 109, 1221
- McNamara, D. H. 2000, Delta Scuti and Related Stars, 210, 373
- McNamara, D. H. 2011, AJ, 142, 110
- Mkrtichian, D. E., Kusakin, A. V., Gamarova, A. Y., & Nazarenko, V. 2002, IAU Colloq. 185: Radial and Nonradial Pulsations as Probes of Stellar Physics, 259, 96
- Mkrtichian, D. E., Nazarenko, V., Gamarova, A. Y., et al. 2003, Interplay of Periodic, Cyclic and Stochastic Variability in Selected Areas of the H-R Diagram, 292, 113
- Palaversa, L., Ivezić, Ž., Eyer, L., et al. 2013, AJ, 146, 101
- Pamyatnykh, A. A. 2000, Delta Scuti and Related Stars, 210, 215
- Pojmanski, G. 1997, Acta Astron., 47, 467
- Pojmanski, G., Pilecki, B., & Szczygiel, D. 2005, Acta Astron., 55, 275
- Prugniel, P., & Soubiran, C. 2001, A&A, 369, 1048
- Prugniel, P., Soubiran, C., Koleva, M., & Le Borgne, D., 2007, arXiv:astro-ph/0703658
- Qian, S.-B., He, J.-J., Zhang, J., et al. 2017a, Research in Astronomy and Astrophysics, 17, 87
- Qian, S.-B., Zhang, J., He, J.-J., Zhu, L.-Y., Zhao, E.-G., Shi, X.-D., Zhou, X., and Han, Z.-T., 2017b, ApJS (submitted)
- Qian, S.-B., Li, L.-J., Wang, S.-M., et al. 2015, AJ, 149, 4
- Qian, S.-B., Liu, N.-P., Li, K., et al. 2013, ApJS, 209, 13
- Qian, S.-B., Wang, J.-J., Zhu, L.-Y., et al. 2014, ApJS, 212, 4
- Qian, S.-B., Yuan, J.-Z., Soonthornthum, B., et al. 2007, ApJ, 671, 811
- Ren, A., Fu, J., De Cat, P., et al. 2016, ApJS, 225, 28
- Rodríguez, E., & Breger, M. 2001, A&A, 366, 178
- Rodríguez, E., López-González, M. J., & López de Coca, P. 2000, A&AS, 144, 469
- Rodríguez, E., & López-González, M. J. 2000, A&A, 359, 597
- Samus', N. N., Kazarovets, E. V., Durlевич, O. V., Kireeva, N. N., & Pamtukhova, E. N. 2017, Astronomy Reports, 61, 80
- Soyduğan, E., İbanoğlu, C., Soyduğan, F., Akan, M. C., & Demircan, O. 2006, MNRAS, 366, 1289

- Straizys, V., & Kuriliene, G. 1981, *Ap&SS*, 80, 353
- Szatmary, K. 1990, *Journal of the American Association of Variable Star Observers (JAAVSO)*, 19, 52
- Szczygieł, D. M., & Fabrycky, D. C. 2007, *MNRAS*, 377, 1263
- Walker, G., Matthews, J., Kuschnig, R., et al. 2003, *PASP*, 115, 1023
- Wang, S.-G., Su, D.-Q., Chu, Y.-Q., Cui, X., & Wang, Y.-N. 1996, *Appl. Opt.*, 35, 5155
- Watson, C. L., Henden, A. A., & Price, A. 2006, *Society for Astronomical Sciences Annual Symposium*, 25, 47
- Woźniak, P. R., Vestrand, W. T., Akerlof, C. W., et al. 2004, *AJ*, 127, 2436
- Wu, Y., Du, B., Luo, A., Zhao, Y., & Yuan, H. 2014, *Statistical Challenges in 21st Century Cosmology*, 306, 340
- Wu, Y., Luo, A.-L., Li, H.-N., et al. 2011b, *RAA*, 11, 924
- Wu, Y., Singh, H. P., Prugniel, P., Gupta, R., & Koleva, M. 2011a, *A&A*, 525, A71
- Yang, S., & Walker, G. A. H. 1986, *PASP*, 98, 862
- Uytterhoeven, K., Moya, A., Grigahcène, A., et al. 2011, *A&A*, 534, A125
- Xiong, D.-R. 1989, *A&A*, 209, 126
- Xiong, D. R., & Deng, L. 2001, *MNRAS*, 324, 243
- Zhao, G., Zhao, Y.-H., Chu, Y.-Q., Jing, Y.-P., & Deng, L.-C. 2012, *Research in Astronomy and Astrophysics*, 12, 723

This paper has been typeset from a $\text{\TeX}/\text{\LaTeX}$ file prepared by the author.